GPR15 facilitates recruitment of regulatory T cells to promote colorectal cancer

Alexandra Adamczyk[1], Eva Pastille[1], Jan Kehrmann[1], Vivian P. Vu[2,3], Robert Geffers[4], Marie-Hélène Wasmer[2,3], Stefan Kasper[5], Martin Schuler[5,6], Christian M. Lange[7], Beat Muggli[8], Tilman T. Rau[2], Diana Klein[9], Wiebke Hansen[1], Philippe Krebs[2], Jan Buer[1] and Astrid M. Westendorf[1,*]

[1]Infection Immunology, Institute of Medical Microbiology, University Hospital Essen, University of Duisburg-Essen, Essen, Germany
[2]Institute of Pathology, University of Bern, Bern, Switzerland
[3]Graduate School for Cellular and Biomedical Sciences, University of Bern, Switzerland
[4]Genome Analytics, Helmholtz Centre for Infection Research, Braunschweig, Germany
[5]Department of Medical Oncology, West German Cancer Center, University Hospital Essen, University of Duisburg-Essen, Essen, Germany
[6]German Cancer Consortium (DKTK), Partner Site University Hospital Essen, Essen, Germany
[7]Department of Gastroenterology and Hepatology, University Hospital Essen, Essen, Germany
[8]Department of Visceral Surgery and Medicine, Inselspital, Bern University Hospital, University of Bern, Bern, Switzerland
[9]Institute for Cell Biology (Cancer Research), University Hospital Essen, University of Duisburg-Essen, Essen, Germany

Running title: GPR15 promotes intestinal tumorigenesis

Keywords: tumor-associated Tregs, GPR15, migration, colorectal cancer, anti-tumor immunity

*Corresponding Author: Astrid M. Westendorf, Infection Immunology, Institute of Medical Microbiology, University Hospital Essen, Hufelandstr. 55, 45122 Essen, Germany. Phone: +492017231826; Fax: +492017235602; E-mail: astrid.westendorf@uk-essen.de

The authors declare no potential conflicts of interest.

Abstract

Colorectal cancer (CRC) is one of the most frequent malignancies worldwide. Despite considerable progress in early detection and treatment, there is still an unmet need for novel anti-tumor therapies, particularly in advanced CRC. Regulatory T cells (Tregs) are increased in the peripheral blood and tumor tissue of CRC patients. Recently, transient ablation of tumor-associated Tregs was shown to foster CD8+ T cell-mediated anti-tumoral immunity in murine CRC models. However, before considering therapies, targeting Tregs in cancer patients and detailed knowledge of the phenotype and features of tumor-associated Tregs is indispensable. Here we demonstrate in a murine model of inflammation-induced CRC that tumor-associated Tregs are mainly of thymic origin and equipped with a specific set of molecules strongly associated with enhanced migratory properties. Particularly, a dense infiltration of Tregs in mouse and human CRC lesions correlated with increased expression of the orphan chemoattractant receptor GPR15 on these cells. Comprehensive gene expression analysis revealed that tumor-associated GPR15+ Tregs have a Th17-like phenotype, thereby producing IL-17 and TNF-α. Gpr15 deficiency repressed Treg infiltration in CRC, which paved the way for enhanced anti-tumoral CD8+ T cell immunity and reduced tumorigenesis. In conclusion, GPR15 represents a promising novel target for modifying T cell-mediated anti-tumoral immunity in CRC.

Statement of Significance

The G protein-coupled receptor 15, an unconventional chemokine receptor, directs regulatory T cells into the colon, thereby modifying the tumor microenvironment and promoting intestinal tumorigenesis.

Introduction

Ongoing colorectal inflammation as it is seen in patients with ulcerative colitis (UC), is strongly associated with the development and progression of colorectal cancer (CRC) (1,2). One hallmark of cancer is the ability to evade the immune system via immunosuppression (3). Therefore, the ratio of pro- and anti-inflammatory immune cells in the tumor microenvironment influences the patients' clinical outcome (4,5). While high density of pro-inflammatory $CD8^+$ cytotoxic T cells and $CD4^+$ helper T cells type 1 (Th1) are clearly associated with a longer disease-free survival of CRC patients (6), the role of $FOXP3^+$ regulatory T cells (Tregs) during CRC is still controversial. Tregs are key mediators of immunoescape and tumor progression, as they are potent suppressors of anti-tumoral immune responses (7). Nevertheless, accumulation of Tregs in the colon of CRC patients was shown to correlate with both, better and worse prognosis (8-11). The origin of tumor-associated Tregs, however, is difficult to distinguish, as both natural occurring Tregs (nTregs) -which originate in the thymus - and peripherally induced Tregs (iTregs) constitutively express the canonical Treg markers FOXP3 and CD25 (12). Many CRC studies on $FOXP3^+$ T cell infiltration have shown showed poor prognosis and lower disease-free survival, while other demonstrated that $FOXP3^+$ T cell infiltration is also associated with a favorable outcome (8-11). Interestingly, studies revealed that these discrepancies may be due to the heterogeneity of FOXP3 expression and the fact that Tregs can show an inflammatory effector T-helper cell phenotype, expressing $FOXP3^{lo}CD45RA^+$, TNF-α, TGF-β and IL-12 (13). In mice, transient ablation of $FOXP3^+$ Tregs has been successfully used to reduce CRC progression (7,14), and targeting Tregs to overcome the suppression of anti-tumor immune responses is thus widely discussed as CRC therapy. However, most of the common therapies are unspecific and have many side effects, not least because Tregs compromise different subpopulations with different functions. Given that Tregs are potent suppressors of inflammation, but simultaneously inhibit anti-tumor immunity, the identification of markers that are exclusively expressed on tumor-associated Tregs would allow to specifically target these cells, without the risk of inducing unwanted side effects.

In this study, we report that the migration of nTregs - rather than the local conversion of naïve T cells into iTregs - underlies the high abundance of tumor-associated Tregs in the colon of CRC mice. In addition, tumor-associated Tregs were characterized by a unique expression of migration receptors. Specifically, we identified G-Protein coupled receptor 15 (GPR15), an unconventional chemokine receptor, preferentially found in the intestinal mucosa, as an important target for the

recruitment of Tregs into the colonic tissue during intestinal tumorigenesis. Finally, *Gpr15* deficiency reduced the infiltration of tumor-associated Tregs in the tumor microenvironment, which boosted anti-tumor immunity and diminished CRC development.

Material and Methods

Mice. All mice were 8 to 12 week-old (mixed-gender and age-matched) when experiments were initiated. Mice were bred and housed in accordance to the guidelines of the Laboratory Animal Facility of the University Hospital Essen. Animal experiments were performed in accordance to the ethical principles and federal guidelines, and approved by the Landesamt für Natur, Umwelt und Verbraucherschutz (LANUV, Germany). BALB/c and C57BL/6 mice were obtained from Envigo RMS GmbH. C.Cg-Foxp3$^{tm2Tch/J}$ (FOXP3-GFP; BALB/c background), Gpr15$^{tm1.1Litt/J}$ (*Gpr15*$^{+/+}$ (WT); *Gpr15*$^{gfp/+}$ (GPR15-GFP, control littermates); *Gpr15*$^{gfp/gfp}$ (KO)) (15) and Foxp3$^{tm1Flv/J}$ (FOXP3-mRFP) mice (both C57BL/6 background) were obtained from the Jackson Laboratory. Crossing GPR15-GFP mice to FOXP3-mRFP mice resulted in GPR15-GFP x FOXP3-mRFP double-reporter mice.

Patient samples. Blood samples were obtained from 13 healthy volunteers and from 19 colon cancer patients. Tissues from tumorous and healthy adjacent colon were provided from 11 CRC patients. Informed written consent was obtained from all patients. Ethical approval was provided by the Medical Faculty of the University of Duisburg-Essen (AZ 05-2882) and the Cantonal Ethics Committee of Bern (2017-01821 and 2018-01502). Fixed human CRC tissues and part of the fresh CRC samples were provided by the Tissue Bank Bern.

Induction of CRC and mouse colonoscopy. CRC was induced using the azoxymethane (AOM) /dextran sulfate sodium (DSS) protocol as described previously (7). Tumor distribution from the first flexure to the anus was determined by murine colonoscopy and tumor sizes were graded from 1-5 as described elsewhere (16). Tumor score per mouse was calculated by summing up the tumor sizes of all tumors in a given mouse. Lymphocyte emigration from the secondary lymphoid organs was blocked using FTY720 (Santa Cruz). In week 8, tumor score of CRC mice was determined by colonoscopy. Mice were separated into two identical groups and 1mg/kg FTY720 was injected intraperitoneally twice a week until week 12.

Generation of bone marrow chimeras. C57BL/6 recipient mice were lethally irradiated with a single dose of 9 Gy, using an Isovolt-320-X-ray machine (Seifert-Pantak). 5×10^6 whole bone marrow (BM) cells from either GPR15-WT (*Gpr15*$^{+/+}$) or GPR15-KO (*Gpr15*$^{gfp/gfp}$) donor mice

were adoptively transfused via i.v. injection and AOM/DSS treatment of chimeras was initiated 8 weeks after BM reconstitution.

Single-cell isolation. Single-cell suspensions from the spleens and mesenteric lymph nodes (mLNs) were prepared by mashing the organs through a 70µm cell strainer using PBS/ 2mM EDTA/ 2% FCS (PAA Laboratories). Mashed spleens were additionally pre-treated with erythrocyte lysis buffer. Murine lamina propria lymphocytes (LPLs) from the intestines were isolated as described previously (7). Blood samples from patients were collected in NH4-Heparin Monovette tubes (Sarstedt). PBMCs were isolated using Biocoll density gradient (Biochrom), washed with PBS/ 2mM EDTA/ 2% FCS and stored in FCS/ 10% DMSO (Carl Roth). Informed written consent was obtained from all patients.

Flow cytometry and cell sorting. Single cells were incubated with fluorochrome-labeled anti-mouse or anti-human antibodies (see Suppl. Table S1). Fixable Viability Dye was used to stain for dead cells. GPR15 expression was determined using GPR15-GFP x FOXP3-mRFP mice and after surface staining, cells were fixed with 2% formaldehyde (Roti®Histofix; Carl Roth). Intracellular staining of FOXP3, Helios, Ki67 and GZMB was performed using the eBioscience™ FOXP3 staining buffer set. To assess IFN-γ, IL-17, IL-10 and TNF-α, cells were stimulated for 4h with 10ng/mL PMA and 1µg/mL ionomycine in the presence of 5µg/mL Brefeldine A and Monensin (1x; Thermo Fisher Scientific) in complete media (IMDMc; IMDM/ 10% FCS/ 2,5µM β-Mercapthoethanol/ 100µg/ml Penicillin/Streptomycin) (all Sigma-Aldrich). After surface staining, cells were fixed with 2% paraformaldehyde, permeabilized with 0.1% NP-40 and stained with antibodies against different cytokines. Flow cytometry analysis of the cells was performed using FACS DIVA software on an LSR II, CANTO, CELESTA or SYMPHONY instrument; cell sorting was performed on a FACS ARIA (all BD Biosciences).

Analysis of the methylation status in the foxp3-TSDR. DNA was isolated from sorted $CD4^+FOXP3^+$ Tregs of healthy and CRC FOXP3-GFP male mice using QIAamp DNA Mini Kit (Qiagen). Bisulphite modification of DNA was performed with BisulFlash DNA Modification Kit (Epigentek). Methylation sensitive real-time PCR was performed as described elsewhere (17). Primer sequences are listed in Suppl. Table S2. Analysis was run on a Roche Light cycler 480 system using Roche TaqMan Probe Master 480 (Roche Diagnostics).

DNA microarray hybridization. Gene expression analysis of FACS-sorted $FOXP3^{+}CD4^{+}$ Tregs from the colonic lamina propria of healthy and CRC mice was performed as described elsewhere (18). For DNA microarray analysis of $GPR15^{+}$ and $GPR15^{-}FOXP3^{+}$ Tregs, 5000 cells were directly sorted into single cell lysis buffer (Thermo Fisher Scientific). Approx. 2ng of total RNA was used for biotin labelling according to the GeneChip® Pico Kit (Affymetrix). 5.5µg of biotinylated cDNAs were fragmented and placed in a hybridization cocktail containing four biotinylated hybridization controls (BioB, BioC, BioD, and Cre). Samples were hybridized to an identical lot of Affymetrix Clariom™ S (400 Format) for 17 hours at 45°C. Hybridization was done for 16 hours at conditions recommended by the manufacturer. Clariom™ S chips were washed and stained in the Affymetrix Fluidics Station 450. GeneChips were scanned by Affymetrix GCS 3000. Image analysis was done by GeneChip® Command Console® Software (AGCC) and Expression Console™ Software (both Affymetrix). Data analysis was performed as described elsewhere (19). Data have been deposited in NCBI's Gene Expression Omnibus and are accessible through GEO Series accession number GSE168744 (https://www.ncbi.nlm.nih.gov/geo/query/acc.cgi?acc=GSE168744).

RNA isolation and quantitative real-time PCR. RNA from murine colonic tissues was isolated using the RNeasy Fibrous Tissue Mini Kit (Qiagen). RNA isolation from sorted single-cell suspensions was performed using the NucleoSpin XS Kit (Macherey-Nagel). Reverse transcription of RNA was performed using M-MLV reverse transcriptase (Promega). Quantitative real-time PCR analysis was performed with an ABI PRISM cycler (Applied Biosystems), using the Fast SYBR Green Master Mix (Thermo Fisher Scientific) and specific primers (see Suppl. Table S2). Relative mRNA levels were calculated with included standard curves for each gene and normalization to the housekeeping gene RPS9.

Colon explant culture and cytokine detection. A small explant (15-25 µg) from the distal part of the colon was cultured for 6h in IMDMc. Cytokine levels in the supernatants were measured by Luminex technology (R&D Systems) on a Luminex 200 instrument using the Luminex IS software (Luminex Corporation). Cytokine concentration were normalized to the respective weight of the colon biopsies.

In-vitro migration assay. GPR15 expression was induced on sorted $CD4^+GPR15^-$ T cells as described previously (15). After 5 days, $CD4^+GPR15^-$ and $CD4^+GPR15^+$ T cells were sorted and subjected to a migration assay using Transwell® chambers (Corning). SDF-1β (50ng/ml; PeproTech)/ IMDMc was added to the bottom chamber. 5×10^5 $GPR15^-$ or $GPR15^+$ cells were added to the upper insert and incubated for 4h at 37°C, after which the migrated cells were collected from the lower chamber and counted. Migration index was calculated as the ratio of migrated cells toward SDF-1β in comparison to cell migrated to media alone.

Short-term competitive in vivo migration assay. GPR15 expression was induced on sorted $CD4^+$ T cells of GPR15-KO mice (*Gpr15*$^{gfp/gfp}$) or control littermates (ctrl, *Gpr15*$^{gfp/+}$) as described previously (15). At day 5, ctrl T cells were stained with cell proliferation dye eFluor™ 670 (Thermo Fisher Scientific) and KO T cells were stained with cell tracker blue CMAC (Thermo Fisher Scientific), mixed at a 1:1 ratio and $1x10^7$ mixed T cells were transferred i.v. into CRC-bearing C57BL/6 recipients. 20h later, cells from the blood, spleen, mLN and the colonic lamina propria were isolated, numbers of KO and ctrl T cells were analyzed via flow cytometry and the ratio of migrated GPR15-expressing versus GPR15-deficient cells were calculated for each compartment.

Tissue microarray (TMA) and pseudo-coloring via color deconvolution. Human CRC tissues were fixed in 4% formaldehyde and embedded in paraffin. Staining reactions were performed by automated staining using a BOND RX autostainer (Leica Biosystems). Sections were first deparaffinized and antigen was retrieved using 1mM Tris solution (pH 9.0) for 40 min at 95°C. Sections were then stained with anti-human GPR15 (1:20; 60 min) and anti-human FOXP3 (1:200; 15 min) antibodies. Antibody binding was visualized using horseradish peroxidase and 3,3-diaminobenzidine (DAB, brown chromogen), or Fast Red (red chromogen), respectively (all Leica Biosystems). The samples were counterstained with hematoxylin and mounted with Aquatex (Merck). Slides were scanned on whole slide scanners Pannoramic 250 Flash (3DHISTECH) or NanoZoomer S360 (Hamamatsu). TMA images were dearrayed using ImageJ (Version 1.52p) and the color deconvolution plugin, resulting in individual channels for GPR15 and FOXP3. Specific threshold was set for GPR15 and FOXP3 and images were pseudo-colored in green (GPR15) and red (FOXP3), respectively, after which images were merged.

Statistical analysis. All analyses were calculated using the GraphPad Prism 7.03 software (La Jolla, USA). Where appropriate, the paired or unpaired Student t-test or Mann Whitney test was used. Differences between means of more than two groups were assessed using one-way ANOVA followed by Dunnett's multiple comparison test. Statistical significance between two groups with different factors was calculated using two-way ANOVA followed by Bonferroni's posttests. Statistical significance was set at $p < 0.05$.

Results

The induction and progression of CRC correlates with the frequency of CD4$^+$ Tregs

Chronic inflammation of the colon is associated with the induction of CRC (20). Using a murine model of CRC based on AOM/DSS (Figure 1 A), we determined intestinal dysplastic changes over time in correlation with colonic Treg frequencies. As early as 4-5 weeks after AOM administration, first dysplastic changes in the colon were identified by colonic endoscopy, and a significant increase in tumor volumes was detected between weeks 7-12, as summarized in the tumor score (Figure 1 B). Concurrently, we observed enhanced frequencies of CD4$^+$FOXP3$^+$ Tregs in week 2 and 5, most likely due to acute inflammation of the colon caused by the DSS administration. From week 7 onwards, the frequency of Tregs in the tumorous tissue increased steadily when compared to healthy colonic tissue, while the frequencies from healthy control (HC) mice increased only minor from week 1 to week 12 (Figure 1 C). Further analysis revealed a positive correlation of the tumor score and colonic Treg frequencies (Figure 1 D).

Tumor-associated Tregs display an nTreg phenotype

We previously established that Tregs are strongly involved in the progression of CRC in mice, as the transient ablation of tumor-associated Tregs improved CD8$^+$ T cell-mediated anti-tumoral immunity (7). Yet, detailed knowledge of the mechanisms underlying Treg accumulation in the colon of CRC mice remained unclear. To define the origin of tumor-associated Tregs, we next analyzed the methylation status of the *foxp3*-Treg-specific demethylated region (*foxp3*-TSDR). Methylation of this genetic region is associated with unstable expression of FOXP3 and commonly found in iTregs or effector T cells, whereas this region is mainly demethylated in thymus-derived nTregs (21). For this, we sort-purified FOXP3-GFP$^+$ Tregs from spleen, mLN and colon of healthy control and CRC FOXP3-GFP reporter mice. As expected, sorted Tregs from the spleen and mLN were mainly demethylated in the *foxp3*-TSDR, confirming the predominantly thymic origin of these cells. This phenotype was independent of CRC (Figure 1 E). Interestingly, Tregs from the colons of healthy mice were mostly methylated in the *foxp3*-TSDR, suggesting a high frequency of intestinal iTregs at steady state (Figure 1 E). On the contrary, CRC-associated Tregs showed a demethylated status (Figure 1 E), hinting at a stable expression of FOXP3 and an nTreg phenotype. The thymic origin of tumor-associated Tregs was further confirmed by an increased expression of the nTreg markers Neuropilin-1 (NRP1) and

Helios (22,23) on tumor-associated Tregs compared to colonic Tregs from control mice (Figure 1 F+G). To get an idea whether the expansion of nTregs in the tumor tissue is based on migration or proliferation, we performed flow cytometry staining for the proliferation markers Ki67 and BrdU. Of note, slightly enhanced expression of Ki67 and BrdU was detected in tumor-associated Tregs compared to Tregs isolated from the colon of healthy control mice (Figure 1 H; Suppl. Fig S1 A+B). However, Ki67 and BrdU expression was also moderately higher in FOXP3$^-$ conventional CD4$^+$ T cells (cCD4$^+$ T cells) of CRC mice compared to healthy control mice (Suppl. Figure S1 C+D). Interestingly, we found increased expression of Treg-associated survival factors, such as IL-2, TNF-α and TGF-β, in the colon of CRC cancer mice compared to HC mice (Suppl. Figure S1 E), but the overall survival of Tregs in the tumorous tissue was rather decreased (Suppl. Figure S1 F), hinting for a balance in proliferation and apoptosis of tumor-associated Tregs. Altogether, these data indicate that CRC-associated Tregs have a thymus-derived origin, which suggests migration of nTregs to and/or proliferation of nTregs in the tumor tissue, rather than a local induction of iTregs.

Unspecific blockade of Treg migration reduces tumor growth in CRC mice

To further address whether Treg migration contributes to Treg accumulation in the colonic tumorous tissue, we next used FTY720 to block the emigration of lymphocytes from secondary lymphoid organs (24) during the time of actual tumor development in AOM/DSS-treated mice (Figure 2 A). Efficacy of FTY720 treatment was verified by analyzing circulating CD4$^+$ and CD8$^+$ T cells (Figure 2 B). Interestingly, FTY720-treated animals showed reduced tumor scores at time of sacrifice (Figure 2 C). Concomitantly, frequencies and numbers of Tregs in the colons were reduced in FTY720-treated CRC mice but not in healthy controls (Figure 2 D). Remarkably, no or only minor alterations in CD8$^+$ and cCD4$^+$ T cell frequencies and numbers were detected in the colonic lamina propria of FTY720-treated and non-treated groups (Figure 2 E, Suppl. Figure S2 A+B). Nevertheless, in CRC mice FTY720 treatment reduced the Treg/ CD8$^+$ T cell ratio and promoted the functional activation of cytotoxic CD8$^+$ T cells (Figure 2 F, G). Thus, our data indicate that Treg migration into the colon promotes CRC tumorigenesis, likely via a shift in the Treg/CD8$^+$ T cell ratio, thereby supporting a pro-tumorigenic milieu.

Tumor-associated Tregs show a specific expression profile for migration receptors

Non-specific blockade of Treg migration reduced the tumor burden in CRC mice and enhanced anti-tumoral immunity. To gain further insights into the molecules supporting nTreg migration to CRC lesions, we next performed global gene expression profiling. FOXP3-GFP$^+$ CD4$^+$ Tregs as well as FOXP3-GFP$^-$ cCD4 were sort-purified from the colon of HC and CRC FOXP3-GFP reporter mice and subjected to microarray analysis. Focusing our analysis on molecules associated with migratory properties, we identified a unique expression pattern on Tregs isolated from colonic tumors (Figure 3 A). In particular, tumor-associated Tregs showed upregulated expression of αv integrins (*Itgav*) as well as the chemokine receptor *Ccr5*, both on transcript and protein level (Figure 3 A+B; Suppl. Figure S3 A+B). Of note, enhanced αv integrins and CCR5 protein expression was restricted to cells isolated from the colon of CRC mice, but the expression was not specific for Tregs (Figure 3 B, Suppl. Figure S3 A+B). Surprisingly, GPR15 was one of the molecules specifically upregulated on tumor-associated Tregs (Figure 3 A). In the past few years, GPR15 gained strong interest in the field of mucosal immunology as a homing receptor for Tregs mainly expressed in the lamina propria of the large intestine (15). Flow cytometry analysis using GPR15-GFP x FOXP3-mRFP double-reporter mice revealed that among CD4$^+$ T cells, GPR15 was preferentially expressed in FOXP3$^+$ cells and more in colonic tumor-associated Tregs than in counterparts from control mice (Figure 3 B+C; Suppl. Figure S3 A). Interestingly, no differences in the expression of GPR15 on a per cell basis was found on GPR15-expressing Tregs (Suppl. Figure S3 B), nor in the expression of GPR15 on colonic CD8$^+$ T cells (Suppl. Figure S3 C-E) from HC and CRC mice. In other organs, such as the small intestine, mLNs and spleen, we did not observe differences in GPR15 expression between control and CRC mice, and nearly no expression of GPR15 was detected on FOXP3$^-$ cCD4$^+$ T cells (Suppl. Figure S4 A+B).

Differential expression of GPR15 in CRC mice

As GPR15 was recently described as a homing receptor for Tregs to the large intestine (15), we next interrogated the possible role of GPR15 for CRC. First, we analyzed whether GPR15 expression in general affects T cell migration. Therefore, GPR15 was induced *in vitro* by stimulation of CD4$^+$ T cells in the presence of IL-2, IL-21, retinoic acid and TGF-β (15) and sort-purified GPR15$^+$ and GPR15$^-$ T cells were subjected to migration assays. Our data revealed that GPR15-expressing cells showed a higher migration capacity than GPR15$^-$ cells (Figure 4 A). Next, we performed GPR15 expression profiling on different immune cell subsets isolated from the colonic lamina propria of CRC mice. In the context of CRC, GPR15 was predominantly

found on FOXP3$^+$ Tregs, whereas only very low or no GPR15 expression was observed on CD8$^+$ T cells, B cells, macrophages (Mph), dendritic cells (DCs), and cCD4$^+$ T cells (Figure 4 B). Furthermore, levels of GPR15 in the colonic mucosa increased over the course of the AOM/DSS treatment compared to naïve conditions (Figure 4 C). Interestingly, *Gpr15* expression correlated with both the tumor score and the numbers of Tregs (Figure 4 D).

To gain further insights on the contribution of GPR15 to the phenotype of tumor-associated Tregs, we performed gene expression analysis of sort-purified GPR15$^+$ and GPR15$^-$ FOXP3$^+$ Tregs from the colon of CRC mice. Compared to GPR15$^-$ counterparts, GPR15$^+$ CRC-associated Tregs showed enhanced expression of 84 genes (Figure 4 E+F). Interestingly, expression of *Ccr5* and *Sell* (L-selectin or CD62L), both of which being genes related to T cell migration, were upregulated in GPR15$^+$ Tregs. Additional genes, such as *Rorc* (Th17 differentiation), *Klrc1* and *Lag3* (immune checkpoint), *Tnfrsf1a* and *Il1r1* (cytokine-cytokine receptor interaction), also showed increased expression in GPR15$^+$ tumor-associated Tregs, while *Il1rl1* (IL-33 receptor) was downregulated in GPR15$^+$ compared to GPR15$^-$ tumor-associated Tregs (Figure 4 E+F). In accordance with the gene expression data, we observed enhanced IL-17 and TNF-α secretion of GPR15$^+$ compared to GPR15$^-$ Tregs, while we found no differences in IFN-γ and IL-10 production between these cell subsets (Figure 4 G). Taken together, these results indicate that CRC-derived GPR15$^+$ Tregs are phenotypically distinct, suggesting that they have distinct functional properties.

Accumulation of GPR15-expressing Tregs in CRC patients

To examine the general relevance of our results from mouse studies, we analyzed GPR15 expression in Tregs from blood and colon tissue samples from CRC patients. Frequencies of FOXP3$^+$CD4$^+$ Tregs and of GPR15-expressing Tregs were enhanced in the blood of CRC patients compared to healthy control donors (Figure 5 A+B), implying that circulating Tregs have a differential expression pattern for GPR15 in CRC patients. Unlike our murine data, we also observed enhanced frequencies of GPR15$^+$ cCD4$^+$ T cells in CRC patients, yet the average percentage of GPR15-expressing cells was higher among Tregs (Figure 5 B). Next, we studied immune cell infiltrates in colon cancer tissues. Compared to adjacent tumor-free tissue, FOXP3$^+$CD4$^+$ Tregs accumulated in CRC lesions (Figure 5 C). In addition, the numbers of GPR15$^+$ Tregs were significantly increased in CRC tissues, contrarily to GPR15$^+$ cCD4$^+$ T cells (Figure 5 D). To strengthen these flow cytometry data, we performed double

immunohistochemistry stainings of human CRC tissues. For better distinction between $FOXP3^+$ (purple, nuclear) and $GPR15^+$ (brown, cytoplasmic) cells, images were dearrayed through pseudo-coloring via color deconvolution. Using this approach, we were able to differentiate $GPR15^+$ cells (green), $FOXP3^+$ (red) and $GPR15^+FOXP3^+$ cells (yellow). In line with the flow cytometry data, GPR15 was detected on both, $FOXP3^+$ and $FOXP3^-$ cells in CRC tissues (Figure 5 E). Of note, not all $FOXP3^+$ cells expressed GPR15 and *vice versa*. In accordance with our data from the mouse model, we observed enhanced secretion of IL-17 and TNF-α in $GPR15^+$ Tregs compared to $GPR15^-$ Tregs from CRC patients, as well as decreased production of IFN-γ (Figure 5 F). In summary, these data suggest that GPR15-expressing Tregs modify the tumor microenvironment in human CRC.

Gpr15-deficiency regulates T cell frequencies and anti-tumoral $CD8^+$ T cell response in colonic tumor tissues

To assess the impact of GPR15 on Treg migration during CRC progression, we applied AOM/DSS treatment to GPR15-KO mice ($Gpr15^{gfp/gfp}$; knock-out) and compared them to GPR15-GFP control littermates ($Gpr15^{gfp/+}$, ctrl) (15). We confirmed *Gpr15* deficiency in these mice by comparing *Gpr15* expression in the colon of GPR15-KO versus control littermates (Figure 6 A). Endoscopic analysis demonstrated that *Gpr15* deficiency results in reduced intestinal tumor burden (Figure 6 B). Importantly, while at steady state the frequencies of Tregs did not differ in the colon of control versus knockout mice, *Gpr15* deficiency resulted in a lower proportion of Tregs in CRC lesions (Figure 6 C+D). Along with the reduced frequencies of Tregs, the Tregs/ $CD8^+$ T cells ration was lower in GPR15-KO CRC mice compared to CRC control littermates (Figure 6 E). In addition, we noticed enhanced functional capacity of $CD8^+$ T cells from GPR15-KO tumors, as illustrated by a larger proportion of $GZMB^+$ $CD8^+$ T cells (Figure 6 F). Recently, we described a connection between IL-33 secretion from colonic explants and extent of CRC in AOM/DSS-treated mice (18). Interestingly, we found here that the secretion of this pro-tumorigenic cytokine was much lower in cancerous tissues from GPR15-KO than in control CRC tissues (Figure 6 G).

Although CRC induction is triggered by inflammatory processes and GPR15 is discussed to be involved in chronic intestinal inflammation (25,26), during acute DSS colitis no differences were found between GPR15-KO and control littermates, neither in disease progression, nor in Treg frequencies and proliferation (Suppl. Figure S5 A-D). These results support the notion that

GPR15 is rather important during the later phase of the AOM/DSS model, when tumors develop and Tregs accumulate in the colonic tissue.

To verify that the reduction of Tregs found in GPR15-KO mice was dependent on reduced migration of GPR15 expressing cells into the colon, we performed a short-term *in vivo* competitive migration experiment. We adoptively transferred equal amounts of fluorescently labeled GPR15-expressing and GPR15-KO cells into C57BL/6 CRC-bearing mice, and then analyzed the distribution of these cells in the different organs. We detected significant more GPR15-expressing than GPR15-deficient cells in the colon of CRC mice, while only minor discrepancies were observed for the other compartments, such as blood, spleen and mLN (Figure 6 H). Finally, lethally irradiated C57BL/6 mice were reconstituted with bone marrow from GPR15-KO or GPR15-WT (*Gpr15*$^{+/+}$*)* littermates and CRC was induced via AOM/DSS treatment. Analysis of blood leukocytes revealed that the bone marrow (BM) reconstitution was successful, as indicated by a clear reduction of GPR15-expressing CD4^{+} T cells in mice reconstituted with GPR15-KO bone marrow (KO => C57BL/6) compared to control chimeras (WT => C57BL/6) (Figure 6 I). Chimeras with GPR15 deficiency in hematopoietic cells showed reduced tumor growth compared to control BM chimeric mice with normal GPR15 expression, which was accompanied by diminished colonic Treg frequencies and numbers (Figure 6 J+K).

In summary, our data demonstrate that GPR15 expression promotes CRC by facilitating the recruitment of Tregs into developing CRC lesions, which in turn impedes the establishment of an effective anti-tumoral CD8^{+} T cell response.

Discussion

Treg frequencies in colonic lesions have strong prognostic properties for CRC patients. Targeting Tregs in the CRC tumor microenvironment might therefore be an effective anti-tumor therapy. However, understanding the specific features of tumor-associated Tregs is strictly necessary to design targeted tumor-specific Treg therapies. In this study, we observed a positive correlation between colonic tumor burden and Treg frequencies in mice and humans with CRC. Moreover, we identified that tumor-associated Tregs are of natural origin and belong to a distinct subpopulation of Tregs, characterized by specific expression of GPR15, participating in the overall enhanced migratory capacity of these cells.

In many types of solid cancers, Tregs outnumber effector T cells in the tumor microenvironment (27-30). While the inflammatory milieu of a tumor may drive the differentiation of $CD4^+$ helper T cells into $FOXP3^+$ iTregs, it has been clearly shown by Malchow *et al* that tumors may also drive the recruitment of preexisting, self-specific nTregs reactive to either ubiquitous or tissue-restricted antigens (31,32). The extent, to which this occurs during CRC, remains poorly described. At steady state, it is considered that about 50% of all Tregs in the colon are peripherally induced Tregs with established tolerance for microbial and nutrient antigens (33). This is well in line with our results, as we observed a strong methylation of the *foxp3*-TSDR locus in colonic Tregs of healthy mice. Contrary, colonic tumor-associated Tregs isolated from AOM/DSS-treated animals were mostly demethylated in the *foxp3*-TSDR, which strongly hints at a stable expression of FOXP3 and an nTreg phenotype. In CRC patients, Zhou and colleagues indeed found high frequencies of Tregs with demethylated *foxp3*-TSDR in the tumor, but also in the adjacent normal tissues. Interestingly, especially the demethylation of *foxp3*-TSDR in Tregs of the adjacent normal tissues correlated with worse survival rates (34). These results raise the question, whether nTregs are recruited to the tumor tissue and/or whether nTregs locally proliferate in response to tumor antigens. As blocking the emigration of Tregs from secondary lymphoid organs reduced the frequencies of tumor-associated Tregs, we conclude that during inflammation-induced CRC, lineage-stable nTregs are recruited into developing tumors. Interestingly, proliferation in tumor-associated Tregs was slightly increased. However, comparing Treg proliferation over the course CRC tumorigenesis, this proliferation appears only to be moderate (Suppl. Figure S1 A). Therefore, we conclude that this moderate rise in proliferation cannot solely explain the strong increase in Treg frequencies we observed in CRC

tissues and rather a combination of both, recruitment and expansion of highly restricted nTregs contribute to the enhanced Treg pool in CRC lesions in our model. To further unravel the exact antigen specificity of tumor-associated Tregs, high throughput analysis on T cell recteptor diversity of CRC-associated Tregs remain to be elucidated in future experiments.

Treg trafficking is regulated by their ability to cross the tumor endothelium, which is promoted by various combinations of chemoattraction and adhesion signals mediated through the expression of distinct chemotactic receptors (35,36). For example, the expression of sphingosine 1 phosphate receptor 1 (S1PR1) on Tregs was shown to be crucial for tumor infiltration (37). In accordance, we observed enhanced expression of S1PR1 on tumor-associated Tregs (Suppl. Figure S6), suggesting that also in our CRC model, Treg migration into the tumorous tissue might be influenced by S1PR1 signaling. Accordingly, blocking S1PR1 signaling by FTY720 mainly influenced Treg infiltration in our system, highlighting the importance of Treg migration to promote colon cancer. In addition, we found a unique transcriptional pattern of migration molecules for CRC-associated Tregs, including expression of classical migration molecules such as CCR5, CCR8, αv and β8 integrins. Nevertheless, enhanced CCR5 and integrin expression was not restricted to Tregs but was also found on effector T cells during CRC. One molecule, which was specifically expressed on colonic Tregs and especially on tumor-associated Tregs in mice, was GPR15. GPR15 was firstly described as an HIV co-receptor with structural homology to other known chemokine receptors (38). Meanwhile, GPR15 was also identified as a receptor involved in the migration of Tregs to the colon but not to the small intestine in mice (15). Recently, we and others demonstrated that GPR15-expressing human T cells show an enhanced migration capacity and that GPR15 expression is altered on $CD4^+$ T cells of UC patients (25,26). In agreement with these findings, we here describe a contribution of GPR15-expressing Tregs to the development and progression of CRC. *Gpr15* deficiency in the context of AOM/DSS treatment resulted in decreased colonic Treg counts that changed the Treg/ $CD8^+$ T cell ratio and a reduced tumor burden. Our data show that this was mediated by immune cells, as mice with *Gpr15* deficiency specifically in the hematopoietic compartment showed a similar phenotype than mice lacking GPR15 in all cells. Of note, the intratumoral ratio of Treg/$CD8^+$ T cell is considered as a crucial prognostic factor for many types of cancers (39,40). Considering that the majority of the immune cells expressing GPR15 in mice are Tregs, we conclude that GPR15 expression directly affects Treg infiltration during CRC, supporting a pro-tumorigenic microenvironment and tumor growth.

GPR15 expression is influenced by the colonic microenvironment, as TGF-β and microbial short chain fatty acids (SCFA) induce GPR15 expression on Tregs (15). The ligand for GPR15 (GPR15L) is expressed by epithelial cells of the gastrointestinal tract (41,42). Additionally, GPR15L is capable of inducing G1 arrest and is therefore discussed as a potential inhibitor of colon cancer cell lines *in vitro* (43). So far, we could not detect any alteration in the expression of *Gpr15L* in the tumor microenvironment compared to healthy tissue (Suppl. Figure S7 A+B), providing evidence that not GPR15-GPR15L interaction alone but an additional mechanism might account for the increased influx of tumor-associated Tregs and their tumor supportive capacity. Indeed, there are some functional differences between $GPR15^+$ and $GPR15^-$ cells. *Ccr5* and *Sell,* both genes associated with T cell migration, were upregulated on $GPR15^+$ tumor-associated Tregs, emphasizing that GPR15-expressing Tregs have a preferable migratory capacity. In fact, we demonstrate that *Gpr15*-deficient cells have a lesser capacity than *Gpr15*-sufficient cells to migrate

from the periphery into the tumorous colonic tissue. Interestingly, enhanced expression of CCR5 on tumor-associated Tregs has been already described, thus CCR5 has been suggested as a potential therapeutic target for Tregs in CRC (44-47). $Ccr5^{-/-}$ mice show delayed tumor growth with an associated reduction in tumor Treg infiltration. However, pharmacological inhibition of CCR5 failed to reduce tumor Treg infiltration in murine tumor models, although it did result in delayed tumor growth in mice and human (46,48). These complex interactions clearly outline the difficulties of targeting single migration molecules in clinical trials and substantiate the need of unraveling the specific features of tumor-associated Tregs in CRC. Detailed knowledge on the exact mechanism how GPR15 expression guides Tregs into the tumor microenvironment, e.g. the expression and/or secretion of GPR15-attracting molecules by tumor cells and/or the tumor microenvironment, and the overall functional consequences of GPR15 expression, still remains to be clarified in more detail.

Generally, the suppressive capacity of Tregs does not seem to be affected by the expression of GPR15 (15). It is more likely that reduced frequencies and numbers of Tregs in CRC lesions account for the enhanced $CD8^+$ T cell-mediated cytotoxic immune response in GPR15-KO compared to control littermates. Still, besides its role in T cell trafficking, GPR15 expression on T cells is associated with enhanced IL-17 secretion (25,49). Consistently, we found enhanced gene expression of *Rorc* and production of IL-17 in $GPR15^+$ tumor-associated Tregs compared to $GPR15^-$ counterparts. Of note, RORγt-expressing tumor-infiltrating Tregs were shown to drive

tumor growth of CRC by controlling IL-6 secretion in DCs (50). Furthermore, IL-17^{+}FOXP3^{+} Tregs accumulate in CRC tissue, express CCR6, TGF-β and IL-6, and significantly suppress CD8^{+} T cell-mediated immunity (51). Just recently Xiong and colleagues described an intricate balance between the aryl hydrocarbon receptor (Ahr)-RORγt-Foxp3 axis in controlling Treg intestinal homing by regulating GPR15 expression under the steady state and during inflammation (52). In our study, we conclude that GPR15 expression firstly enables trafficking of Tregs into colonic tumor tissues and secondly identifies a potentially tumor-promoting Th17-like Treg population. Of note, we also found that compared to GPR15^{-} Tregs, GPR15^{+} Tregs secreted more TNF-α, which has been reported to support Treg expansion, stability and functions, thereby supporting tumor growth (53).

Recently, we demonstrated that ST2 expression modulates the phenotype of Tregs to promote intestinal cancer (18). Interestingly, gene expression of *Il1rl1*, which counts for the IL-33 receptor ST2, was downregulated on GPR15^{+} Tregs compared to GPR15^{-} tumor-associated Tregs. Although we found co-expression of GPR15 and ST2 on tumor-associated Tregs in mice and humans, the majority of ST2^{+} Tregs did not express GPR15 (Suppl. Figure S8 A+B), providing evidence that GPR15^{+} Tregs belong to a specific migratory subpopulation of Tregs and that these cells, at least partially, might differ from ST2^{+} Tregs. Interestingly, *Gpr15* deficiency resulted in reduced tumor-promoting IL-33 secretion in the colon of CRC mice, hinting for an interaction between GPR15 expression and the IL-33/ST2 pathway. Therefore, we assume that conjoint blockade of the GPR15-mediated migration of tumor-associated Tregs and of the IL-33/ST2 inflammatory pathway might represent a valid therapeutic strategy to specifically tackle a large proportion of Tregs during CRC.

In conclusion, our findings support the idea that GPR15 presents a promising novel therapeutic target for the treatment of CRC and provide fresh insights into the complexity of Treg migration and the interaction to other immune cells during intestinal tumorigenesis.

Acknowledgements

We acknowledge Christian Fehring, Witold Bartosik Mechthild Hemmler-Roloff and Christina Liebig for their excellent technical support. We are further grateful to Kristýna Hlavačková for experimental support, as well as to the team of the Translational Research Unit of the Institute of Pathology in Bern. We thank Daniela Catrini for the critical reading of the manuscript. This work was supported by the BIOME-PEP program of the Medical Faculty, University of Duisburg-Essen (to AA) and the Helmut Horten Foundation (to PK).

Author's contributions

AA and AMW designed all experiments. AA performed most of the experiments and data analysis. EP, JK, RG, TTR, MHW, VPV, BM and DK supported the experiments. MS and SK provided the patients' blood samples. PK and CML coordinated and supervised the experiments and the data involving tissues from CRC patients. AA and AMW wrote the manuscript. JB, PK, MS, SK, WH and EP revised the manuscript.

References

1. Olen O, Erichsen R, Sachs MC, Pedersen L, Halfvarson J, Askling J, *et al.* Colorectal cancer in ulcerative colitis: a Scandinavian population-based cohort study. Lancet **2020**;395:123-31
2. Grivennikov SI, Wang K, Mucida D, Stewart CA, Schnabl B, Jauch D, *et al.* Adenoma-linked barrier defects and microbial products drive IL-23/IL-17-mediated tumour growth. Nature **2012**;491:254-8
3. Hanahan D, Weinberg RA. Hallmarks of cancer: the next generation. Cell **2011**;144:646-74
4. Fridman WH, Pages F, Sautes-Fridman C, Galon J. The immune contexture in human tumours: impact on clinical outcome. Nat Rev Cancer **2012**;12:298-306
5. deLeeuw RJ, Kost SE, Kakal JA, Nelson BH. The prognostic value of FoxP3+ tumor-infiltrating lymphocytes in cancer: a critical review of the literature. Clin Cancer Res **2012**;18:3022-9
6. Galon J, Costes A, Sanchez-Cabo F, Kirilovsky A, Mlecnik B, Lagorce-Pages C, *et al.* Type, density, and location of immune cells within human colorectal tumors predict clinical outcome. Science **2006**;313:1960-4
7. Pastille E, Bardini K, Fleissner D, Adamczyk A, Frede A, Wadwa M, *et al.* Transient ablation of regulatory T cells improves antitumor immunity in colitis-associated colon cancer. Cancer Res **2014**;74:4258-69
8. Le Gouvello S, Bastuji-Garin S, Aloulou N, Mansour H, Chaumette MT, Berrehar F, *et al.* High prevalence of Foxp3 and IL17 in MMR-proficient colorectal carcinomas. Gut **2008**;57:772-9
9. Ling KL, Pratap SE, Bates GJ, Singh B, Mortensen NJ, George BD, *et al.* Increased frequency of regulatory T cells in peripheral blood and tumour infiltrating lymphocytes in colorectal cancer patients. Cancer Immun **2007**;7:7
10. Salama P, Phillips M, Grieu F, Morris M, Zeps N, Joseph D, *et al.* Tumor-infiltrating FOXP3+ T regulatory cells show strong prognostic significance in colorectal cancer. J Clin Oncol **2009**;27:186-92
11. Sinicrope FA, Rego RL, Ansell SM, Knutson KL, Foster NR, Sargent DJ. Intraepithelial effector (CD3+)/regulatory (FoxP3+) T-cell ratio predicts a clinical outcome of human colon carcinoma. Gastroenterology **2009**;137:1270-9
12. Josefowicz SZ, Lu LF, Rudensky AY. Regulatory T cells: mechanisms of differentiation and function. Annu Rev Immunol **2012**;30:531-64
13. Saito T, Nishikawa H, Wada H, Nagano Y, Sugiyama D, Atarashi K, *et al.* Two FOXP3(+)CD4(+) T cell subpopulations distinctly control the prognosis of colorectal cancers. Nat Med **2016**;22:679-84
14. Szeponik L, Akeus P, Rodin W, Raghavan S, Quiding-Jarbrink M. Regulatory T cells specifically suppress conventional CD8alphabeta T cells in intestinal tumors of APC(Min/+) mice. Cancer Immunol Immunother **2020**
15. Kim SV, Xiang WV, Kwak C, Yang Y, Lin XW, Ota M, *et al.* GPR15-mediated homing controls immune homeostasis in the large intestine mucosa. Science **2013**;340:1456-9
16. Becker C, Fantini MC, Neurath MF. High resolution colonoscopy in live mice. Nat Protoc **2006**;1:2900-4
17. Tatura R, Zeschnigk M, Hansen W, Steinmann J, Vidigal PG, Hutzler M, *et al.* Relevance of Foxp3(+) regulatory T cells for early and late phases of murine sepsis. Immunology **2015**;146:144-56
18. Pastille E, Wasmer MH, Adamczyk A, Vu VP, Mager LF, Phuong NNT, *et al.* The IL-33/ST2 pathway shapes the regulatory T cell phenotype to promote intestinal cancer. Mucosal Immunol **2019**;12:990-1003
19. Smyth GK. Linear models and empirical bayes methods for assessing differential expression in microarray experiments. Stat Appl Genet Mol Biol **2004**;3:Article3

20. Lasry A, Zinger A, Ben-Neriah Y. Inflammatory networks underlying colorectal cancer. Nat Immunol **2016**;17:230-40
21. Floess S, Freyer J, Siewert C, Baron U, Olek S, Polansky J, *et al.* Epigenetic control of the foxp3 locus in regulatory T cells. PLoS Biol **2007**;5:e38
22. Sugimoto N, Oida T, Hirota K, Nakamura K, Nomura T, Uchiyama T, *et al.* Foxp3-dependent and -independent molecules specific for CD25+CD4+ natural regulatory T cells revealed by DNA microarray analysis. Int Immunol **2006**;18:1197-209
23. Yadav M, Louvet C, Davini D, Gardner JM, Martinez-Llordella M, Bailey-Bucktrout S, *et al.* Neuropilin-1 distinguishes natural and inducible regulatory T cells among regulatory T cell subsets in vivo. J Exp Med **2012**;209:1713-22, S1-19
24. Chiba K. FTY720, a new class of immunomodulator, inhibits lymphocyte egress from secondary lymphoid tissues and thymus by agonistic activity at sphingosine 1-phosphate receptors. Pharmacol Ther **2005**;108:308-19
25. Adamczyk A, Gageik D, Frede A, Pastille E, Hansen W, Rueffer A, *et al.* Differential expression of GPR15 on T cells during ulcerative colitis. JCI Insight **2017**;2
26. Nguyen LP, Pan J, Dinh TT, Hadeiba H, O'Hara E, 3rd, Ebtikar A, *et al.* Role and species-specific expression of colon T cell homing receptor GPR15 in colitis. Nat Immunol **2015**;16:207-13
27. Nagase H, Takeoka T, Urakawa S, Morimoto-Okazawa A, Kawashima A, Iwahori K, *et al.* ICOS(+) Foxp3(+) TILs in gastric cancer are prognostic markers and effector regulatory T cells associated with Helicobacter pylori. Int J Cancer **2017**;140:686-95
28. Akimova T, Zhang T, Negorev D, Singhal S, Stadanlick J, Rao A, *et al.* Human lung tumor FOXP3+ Tregs upregulate four "Treg-locking" transcription factors. JCI Insight **2017**;2
29. Tang Y, Xu X, Guo S, Zhang C, Tang Y, Tian Y, *et al.* An increased abundance of tumor-infiltrating regulatory T cells is correlated with the progression and prognosis of pancreatic ductal adenocarcinoma. PLoS One **2014**;9:e91551
30. Vence L, Palucka AK, Fay JW, Ito T, Liu YJ, Banchereau J, *et al.* Circulating tumor antigen-specific regulatory T cells in patients with metastatic melanoma. Proc Natl Acad Sci U S A **2007**;104:20884-9
31. Malchow S, Leventhal DS, Nishi S, Fischer BI, Shen L, Paner GP, *et al.* Aire-dependent thymic development of tumor-associated regulatory T cells. Science **2013**;339:1219-24
32. Savage PA, Leventhal DS, Malchow S. Shaping the repertoire of tumor-infiltrating effector and regulatory T cells. Immunol Rev **2014**;259:245-58
33. Sharma A, Rudra D. Emerging Functions of Regulatory T Cells in Tissue Homeostasis. Front Immunol **2018**;9:883
34. Zhuo C, Li Z, Xu Y, Wang Y, Li Q, Peng J, *et al.* Higher FOXP3-TSDR demethylation rates in adjacent normal tissues in patients with colon cancer were associated with worse survival. Mol Cancer **2014**;13:153
35. Facciabene A, Motz GT, Coukos G. T-regulatory cells: key players in tumor immune escape and angiogenesis. Cancer Res **2012**;72:2162-71
36. Adams DH, Eksteen B. Aberrant homing of mucosal T cells and extra-intestinal manifestations of inflammatory bowel disease. Nat Rev Immunol **2006**;6:244-51
37. Priceman SJ, Shen S, Wang L, Deng J, Yue C, Kujawski M, *et al.* S1PR1 is crucial for accumulation of regulatory T cells in tumors via STAT3. Cell Rep **2014**;6:992-9
38. Blaak H, Boers PH, Gruters RA, Schuitemaker H, van der Ende ME, Osterhaus AD. CCR5, GPR15, and CXCR6 are major coreceptors of human immunodeficiency virus type 2 variants isolated from individuals with and without plasma viremia. J Virol **2005**;79:1686-700
39. Ostroumov D, Fekete-Drimusz N, Saborowski M, Kuhnel F, Woller N. CD4 and CD8 T lymphocyte interplay in controlling tumor growth. Cell Mol Life Sci **2018**;75:689-713
40. Pages F, Mlecnik B, Marliot F, Bindea G, Ou FS, Bifulco C, *et al.* International validation of the consensus Immunoscore for the classification of colon cancer: a prognostic and accuracy study. Lancet **2018**;391:2128-39

41. Ocon B, Pan J, Dinh TT, Chen W, Ballet R, Bscheider M, *et al.* A Mucosal and Cutaneous Chemokine Ligand for the Lymphocyte Chemoattractant Receptor GPR15. Front Immunol **2017**;8:1111
42. Suply T, Hannedouche S, Carte N, Li J, Grosshans B, Schaefer M, *et al.* A natural ligand for the orphan receptor GPR15 modulates lymphocyte recruitment to epithelia. Sci Signal **2017**;10
43. Pan W, Cheng Y, Zhang H, Liu B, Mo X, Li T, *et al.* CSBF/C10orf99, a novel potential cytokine, inhibits colon cancer cell growth through inducing G1 arrest. Sci Rep **2014**;4:6812
44. Chang LY, Lin YC, Mahalingam J, Huang CT, Chen TW, Kang CW, *et al.* Tumor-derived chemokine CCL5 enhances TGF-beta-mediated killing of CD8(+) T cells in colon cancer by T-regulatory cells. Cancer Res **2012**;72:1092-102
45. Schlecker E, Stojanovic A, Eisen C, Quack C, Falk CS, Umansky V, *et al.* Tumor-infiltrating monocytic myeloid-derived suppressor cells mediate CCR5-dependent recruitment of regulatory T cells favoring tumor growth. J Immunol **2012**;189:5602-11
46. Ward ST, Li KK, Hepburn E, Weston CJ, Curbishley SM, Reynolds GM, *et al.* The effects of CCR5 inhibition on regulatory T-cell recruitment to colorectal cancer. Br J Cancer **2015**;112:319-28
47. You Y, Li Y, Li M, Lei M, Wu M, Qu Y, *et al.* Ovarian cancer stem cells promote tumour immune privilege and invasion via CCL5 and regulatory T cells. Clin Exp Immunol **2018**;191:60-73
48. Halama N, Zoernig I, Berthel A, Kahlert C, Klupp F, Suarez-Carmona M, *et al.* Tumoral Immune Cell Exploitation in Colorectal Cancer Metastases Can Be Targeted Effectively by Anti-CCR5 Therapy in Cancer Patients. Cancer Cell **2016**;29:587-601
49. Ammitzboll C, von Essen MR, Bornsen L, Petersen ER, McWilliam O, Ratzer R, *et al.* GPR15(+) T cells are Th17 like, increased in smokers and associated with multiple sclerosis. J Autoimmun **2019**;97:114-21
50. Rizzo A, Di Giovangiulio M, Stolfi C, Franze E, Fehling HJ, Carsetti R, *et al.* RORgammat-Expressing Tregs Drive the Growth of Colitis-Associated Colorectal Cancer by Controlling IL6 in Dendritic Cells. Cancer Immunol Res **2018**;6:1082-92
51. Li L, Boussiotis VA. The role of IL-17-producing Foxp3+ CD4+ T cells in inflammatory bowel disease and colon cancer. Clin Immunol **2013**;148:246-53
52. Xiong L, Dean JW, Fu Z, Oliff KN, Bostick JW, Ye J, *et al.* Ahr-Foxp3-RORgammat axis controls gut homing of CD4(+) T cells by regulating GPR15. Sci Immunol **2020**;5
53. Salomon BL, Leclerc M, Tosello J, Ronin E, Piaggio E, Cohen JL. Tumor Necrosis Factor alpha and Regulatory T Cells in Oncoimmunology. Front Immunol **2018**;9:444

Figure Legends

Figure 1. High abundance of colonic Tregs correlates with tumor progression and a natural origin of tumor-associated Tregs. (A) Schematic illustration of the azoxymethane (AOM)/ dextran sodium sulfate salt (DSS) protocol used for the induction of colorectal cancer (CRC) in naïve BALB/c mice (B-D, F-H) or FOXP3-GFP mice (E). After a single administration of AOM, mice received tree cycles of 3 % DSS in the drinking water. Analysis was performed on week 1, 2, 4, 5, 7, 8, and 10 to 12. (B) Tumor size and numbers were analyzed by colonoscopy from which tumor score was calculated. (C) Frequency of $FOXP3^{+}CD4^{+}$ regulatory T cells (Tregs) in the colonic lamina propria from healthy control (HC; n=1-3 per week and experiment) and CRC-bearing mice (n=3-4 per week and experiment) was determined by flow cytometry. Data represent mean ± SEM of 2-3 individual experiments. Statistical analyses were performed by one-way ANOVA, followed by Dunnett's multiple comparison test. (D) Correlation analysis between Treg frequencies in the colon and the tumor score of CRC mice. Line represents linear regression of correlation with Pearson r coefficient. (E) $FOXP3^{+}CD4^{+}$ Tregs from different organs of HC and CRC Foxp3-GFP mice were sort-purified on week 12 for methylation studies. Heat-map showing mean percentage of methylation of the *foxp3*-TSDR (Treg Specific Demethylated Region) from two individual experiments. In weeks 10 to 12, expression of (G) Neuropilin 1 (NRP1) and (H) Helios and (F) Ki67, was analyzed by flow cytometry in $FOXP3^{+}CD4^{+}$ Tregs from the spleen, mesenteric lymph nodes (mLN) and the colon of HC (n=10-26) and CRC (n=23-44) mice. Data show means ± SEM of 4-9 individual experiments. Statistical analysis was performed by two-way ANOVA and Bonferroni's multiple comparison test. * $P < 0.05$; ***$P < 0.001$;****$P < 0.0001$; ns = not significant

Figure 2. Unspecific blocking of lymphocyte emigration with FTY720 reduces CRC tumorigenesis. (A) Schematic time schedule of FTY720 administration during AOM/DSS treatment of BALB/c mice. After the last DSS cycle in week 8, the lymphocyte emigration from secondary lymphatic organs was blocked via intraperitoneal (i.p.) injection of FTY720 (1mg/kg of body weight; twice a week) in CRC and healthy control mice (HC). (B) Frequency of $CD4^+$ and $CD8^+$ T cells in the blood from FTY720 treated (+) and untreated (-) HC and CRC mice was analyzed by flow cytometry. (C) In week 8 (before FTY720 treatment) and in week 12 tumor sizes and numbers were analyzed by endoscopy and tumor score was calculated. Representative endoscopic pictures from FTY720 treated and untreated CRC mice in week 12 are depicted below. Frequencies and absolute numbers of (D) $FOXP3^+CD4^+$ Tregs and (E) $CD8^+$ T cells in the colon of FTY720 treated (+) and untreated (-) HC and CRC mice were analyzed via flow cytometry. (F) The Tregs/ $CD8^+$ T cell ratio was calculated from the absolute cell numbers of Treg and $CD8^+$ T cells in the colonic lamina propria. (G) Representative plots of intracellular flow cytometry analysis of GZMB and IFN-γ production in $CD8^+$ T cells. Data show means ± SEM of 3 individual experiments; HC n= 8-10; CRC n=9-12. Statistical analysis was performed using (C) Student's t-test or (B,D-F) two-way ANOVA, followed by Bonferroni's multiple comparison test. * $P < 0.05$; ***$P < 0.001$; ns = not significant

Figure 3. Tumor-associated Tregs have a specific migratory phenotype. (A) Gene expression profiling of migration molecules from sorted colonic tumor-associated Tregs ($FOXP3^+$) and $FOXP3^-$ $CD4^+$ T cells from colitis-associated colon cancer (CRC) FOXP3-GFP mice and untreated healthy control littermates (HC) was performed in week 10-12 after AOM/DSS administration. Average expression of genes related to cell migration is depicted in the heat map as fold change from -5 (green) to +5 (red). (B) Flow cytometry analysis of CCR5, αv integrin, and GPR15 expression on $FOXP3^+$ Tregs and $FOXP3^-$ conventional $CD4^+$ T cells ($cCD4^+$ T cells) from CRC and HC mice in week 10-12 are shown as means ± SEM of 2-3 individual experiments; HC n=8-11; CRC n=11-19. BALB/c mice were used for CCR5 and αv integrin analysis. For GPR15 expression analysis, GPR15-GFP x FOXP3-RFP double-reporter mice were used. (C) Representative flow cytometry plots for GPR15 expression on $CD4^+$ T cells are shown. Statistical analysis was performed using Student's t-test. $^{**}P < 0.01$; $^{****}P < 0.0001$, ns = not significant

Figure 4. Differential GPR15-expression on tumor-associated Tregs correlates with tumor progression and constitutes a Treg subpopulation with specific migratory and functional features. (A) GPR15 was induced on $CD4^+$ T cells for 5 days using GPR15-GFP ($GPR15^{gfp/+}$) mice. $GPR15^+$ and $GPR15^-$ cells were sorted and migration assay towards SDF-1β was performed on transwell system. Data show summary of means ± SEM of 5 individual experiments; n=13-15. (B) CRC was induced in FOXP3-GFP mice. Tumor-associated $FOXP3^+CD4^+$ Tregs, $FOXP3^-$ conventional $CD4^+$ T cells (cCD4$^+$ T cells), $CD8^+CD11c^-eGFP^-$ ($FOXP3^-$) T cells ($CD8^+$ T cells), $B220^+CD11c^-eGFP^-$ ($FOXP3^-$) cells (B cells), $CD11b^+F4/80^+$ $CD11c^{int}$ macrophages (Mph), and $CD11b^+$ $CD11c^+$ $F4/80^-$ dendritic cells (DCs) were sorted from the colon of CRC mice, and relative expression of *Gpr15*, in the lamina propria mononuclear cells (LPMCs), was measured by qRT-PCR. (C) Expression of *Gpr15* in colon biopsies of healthy control (HC) and CRC BALB/c mice was determined by qRT-PCR over the time course of the AOM/DSS treatment (week 1-12). Expression levels were normalized to relative expression of HC. Data show summary of means ± SEM of 2 individual experiments. (D) Correlation between *Gpr15* expression in the colon and tumor score (left panel) or absolute numbers of $FOXP3^+CD4^+$Tregs (right panel) were determined. Lines represent linear regression of correlation with Pearson r coefficient. (E, F) CRC was induced in three FOXP3-mRFP x GPR15-GFP double reporter mice. $GPR15\text{-}GFP^+$ versus $GPR15\text{-}GFP^-$ tumor-associated Tregs (RFP^+) were sorted from the tumorous colonic lamina propria and analyzed by microarray. (E) Volcano plot of differential gene expression patterns between $GPR15^+$ and $GPR15^-$ tumor-associated Tregs. Grey dots represent differentially expressed genes with adjusted p-value (10 genes downregulated and 84 genes upregulated). (F) Differential gene expression of selected genes for $GPR15^+$ and $GPR15^-$ tumor-associated Tregs. (G) $GPR15^+$ and $GPR15^-$ T cells were sorted from the spleen of CRC and HC FOXP3-GFP mice, restimulated with PMA and Ionomycin and cytokine secretion of IL-17, TNF-α, IFN-γ and IL-10 on $FOXP3^+$ Tregs were determined by flow cytometry. Statistical analysis was performed using (A, G) two-way ANOVA, followed by Bonferroni's multiple comparison test or (C) one-way ANOVA followed by Dunnett's multiple comparisons test. * $P < 0.05$; ** $P < 0.01$; **** $P < 0.0001$; ns = not significant

Figure 5. Differential expression of GPR15 in CRC patients. (A, B) PBMCs from healthy control donors (HC, n=13) and colorectal cancer patients (CRC, n=19) were stained for (A) FOXP3 on $CD4^+$ T cells and (B) GPR15 on $FOXP3^+CD4^+$ Tregs and $FOXP3^-$ conventional $CD4^+$ T cells ($cCD4^+$ T cells). Expression is demonstrated as median (horizontal lines), 25^{th} to 75^{th} percentile (extension of boxes) and range (error bars). (C, D) Tumorous (T) and adjacent non-tumorous (N) colonic tissues from 11 CRC patients were stained for (C) FOXP3 on $CD4^+$ T cells or (D) GPR15 on $FOXP3^+CD4^+$ Tregs and $FOXP3^-$ $cCD4^+$ T cells, and cell numbers were determined per gram of tissue. Statistical analysis was performed using paired Student's t-test. (E) Immunohistochemistry stainings (H&E) of human CRC lesion show co-expression of FOXP3 (purple) and GPR15 (brown) on cells indicated by arrowheads. Images were dearrayed via color deconvolution and pseudocolored (PC) into $GPR15^+$ cells (green), $FOXP3^+$ cells (red), or $GPR15^+FOXP3^+$ (yellow). Merged images (left panel) and single PC images (right panel). (F) $GPR15^+$ and $GPR15^-$ $CD4^+$ T cells were sorted from PBMCs of 20 CRC patients, stimulated for 3 days with αCD3 and αCD28, restimulated with PMA and Ionomycine, and cytokine production of IL-17, TNF-α, IFN-γ and IL-10 on $FOXP3^+$ Tregs was determined by flow cytometry. Statistical analysis was performed using (A, B) Mann-Whitney test or (C, D, F) paired Student's t-test. * $P < 0.05$; ** $P < 0.01$; ns = not significant

Figure 6. Reduced tumor growth in GPR15-KO mice is associated with low frequency of tumor-infiltrating Tregs and enhanced anti-tumoral CD8$^+$ T cell immunity. (A-G) CRC was induced in GPR15-KO (knock-out; *Gpr15*$^{gfp/gfp}$) or control littermates (ctrl, *Gpr15*$^{gfp/+}$). Analysis was performed after cancer induction at week 10-12. (A) Relative expression of *Gpr15* in the colon of AOM/DSS-treated KO (n=8) or ctrl littermates (n=8) was determined by qRT-PCR. n.d. = not detectable. (B) Tumor size and numbers in KO and control littermates were analyzed by colonoscopy, and tumor score for each individual mouse was calculated. Representative endoscopic pictures from the tumor distribution of KO and control littermates are shown. (C-F) Lymphocytes were isolated from the colonic lamina propria of KO and control littermates, and (C) frequencies and (D) absolute cell number of FOXP3$^+$CD4$^+$ T cells; or (F) frequencies of Granzyme B$^+$ (GZMB) CD8$^+$ T cells were measured by flow cytometry. Representative dot plots of GZMB$^+$ CD8$^+$ T cells from AOM/DSS-treated WT and KO mice are depicted in (F). (E) The Tregs/ CD8$^+$ T cell ratio was calculated from the absolute cell numbers of Treg and CD8$^+$ T cells in the colonic lamina propria of HC and CRC mice. (G) IL-33 secretion from colonic tissue explants. Data show means ± SEM from 5 individual experiments, HC; n=10-12 and CRC; n= 18-20. (H) GPR15 was induced in sorted CD4$^+$ T cells from GPR15-KO (KO, *Gpr15*$^{gfp/gfp}$) mice or control littermates (ctrl, *Gpr15*$^{gfp/+}$). Cells were fluorescently labeled, transferred at equal amounts into CRC-bearing C57BL/6 mice (n=6) and the ratio of ctrl/ KO cells in the different compartments was analyzed via flow cytometry. (I-K) C57BL/6 mice were lethally irradiated, reconstituted with bone marrow from GPR15-KO (*Gpr15*$^{gfp/gfp}$; KO => C57BL/6, n=10) or GPR15-WT littermates (*Gpr15*$^{+/+}$, WT => C57BL/6, n=10), treated with AOM/ DSS and analyzed in week 10 after AOM administration. (I) Frequency of GPR15$^+$CD4$^+$ T cells in the blood was determined by flow cytometry. (J) Tumor size and numbers in mice were analyzed by colonoscopy, and tumor score for each individual mouse was calculated. Representative endoscopic pictures from the tumor distribution of WT => C57BL/6 and KO => C57BL/6 are shown. (K) Frequencies and absolute numbers of FOXP3$^+$CD4$^+$ Tregs in the colon of WT => C57BL/6 and KO => C57BL/6 mice were measured by flow cytometry. Statistical analysis was performed using (B, F, I-K) Students's t-test, (C-E, G), two-way ANOVA followed by Bonferroni's multiple comparison test or (H) one-way ANOVA followed by Dunnett's multiple comparisons test. * $P < 0.05$; ** $P < 0.01$; *** $P < 0.001$; **** $P < 0.0001$; ns = not significant

Author Manuscript Published OnlineFirst on March 16, 2021; DOI: 10.1158/0008-5472.CAN-20-2133
Author manuscripts have been peer reviewed and accepted for publication but have not yet been edited.

Adamczyk et al., Figure 1

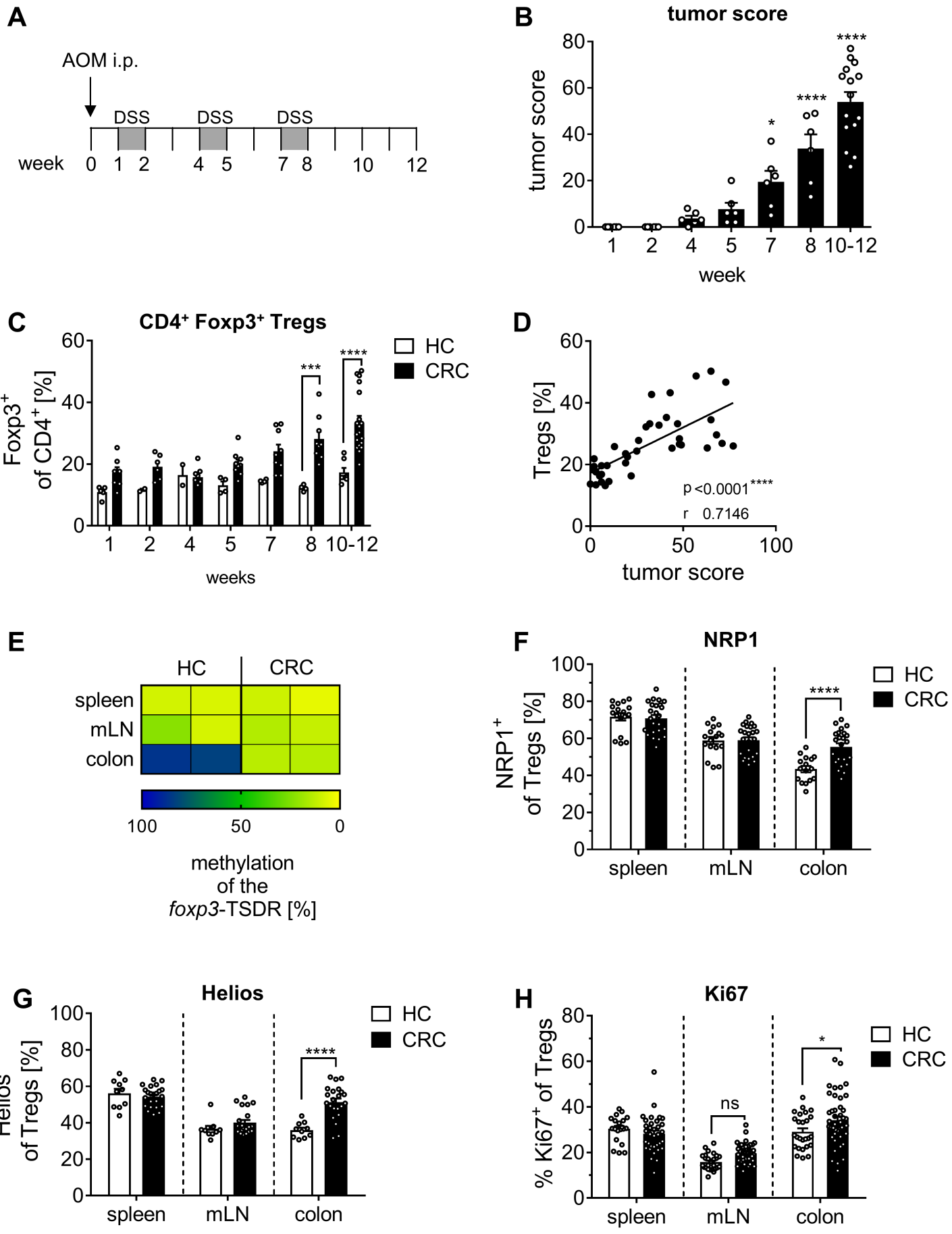

Author Manuscript Published OnlineFirst on March 16, 2021; DOI: 10.1158/0008-5472.CAN-20-2133
Author manuscripts have been peer reviewed and accepted for publication but have not yet been edited.

Adamczyk et al., Figure 2

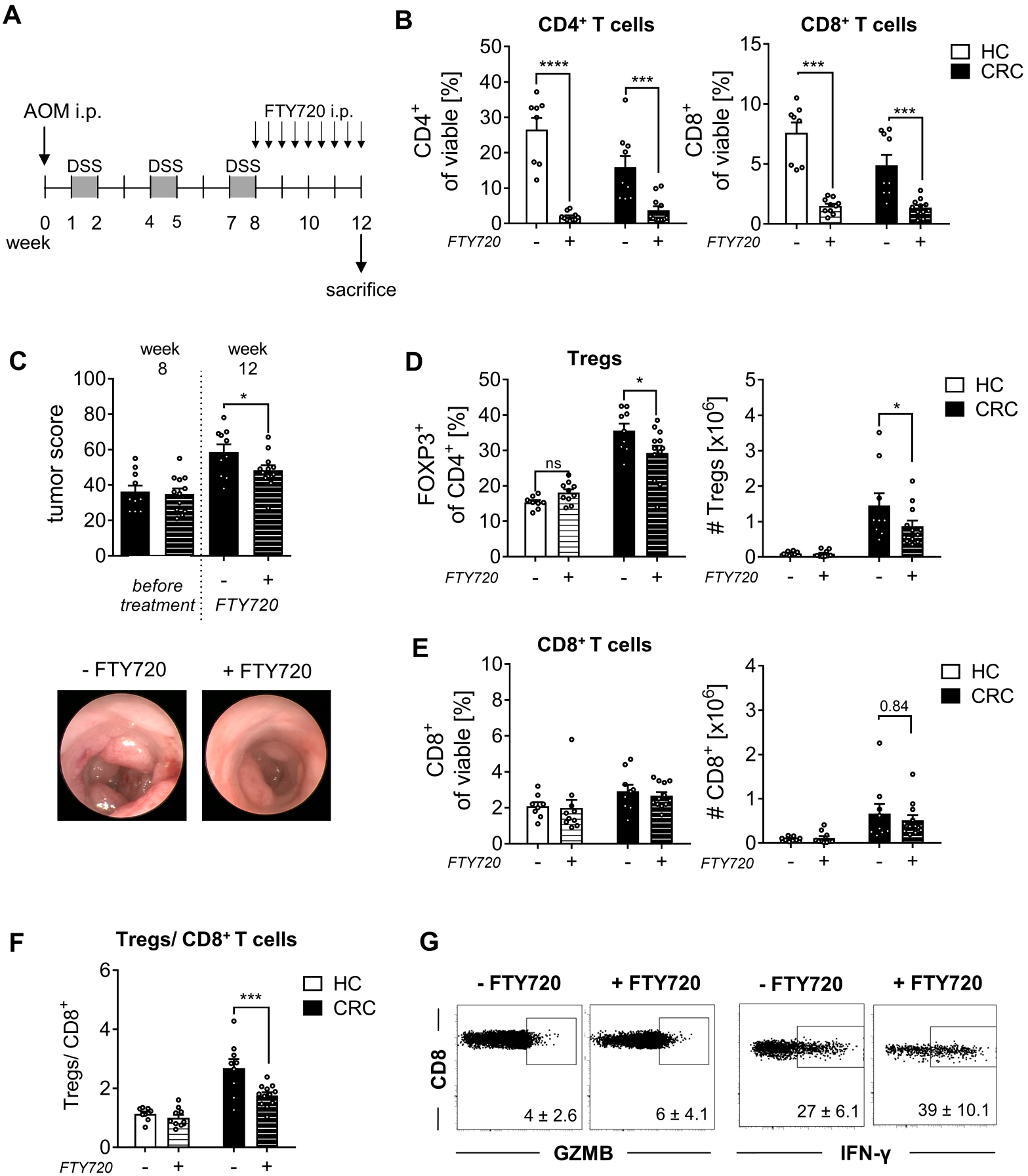

Author Manuscript Published OnlineFirst on March 16, 2021; DOI: 10.1158/0008-5472.CAN-20-2133
Author manuscripts have been peer reviewed and accepted for publication but have not yet been edited.

Adamczyk et al., Figure 3

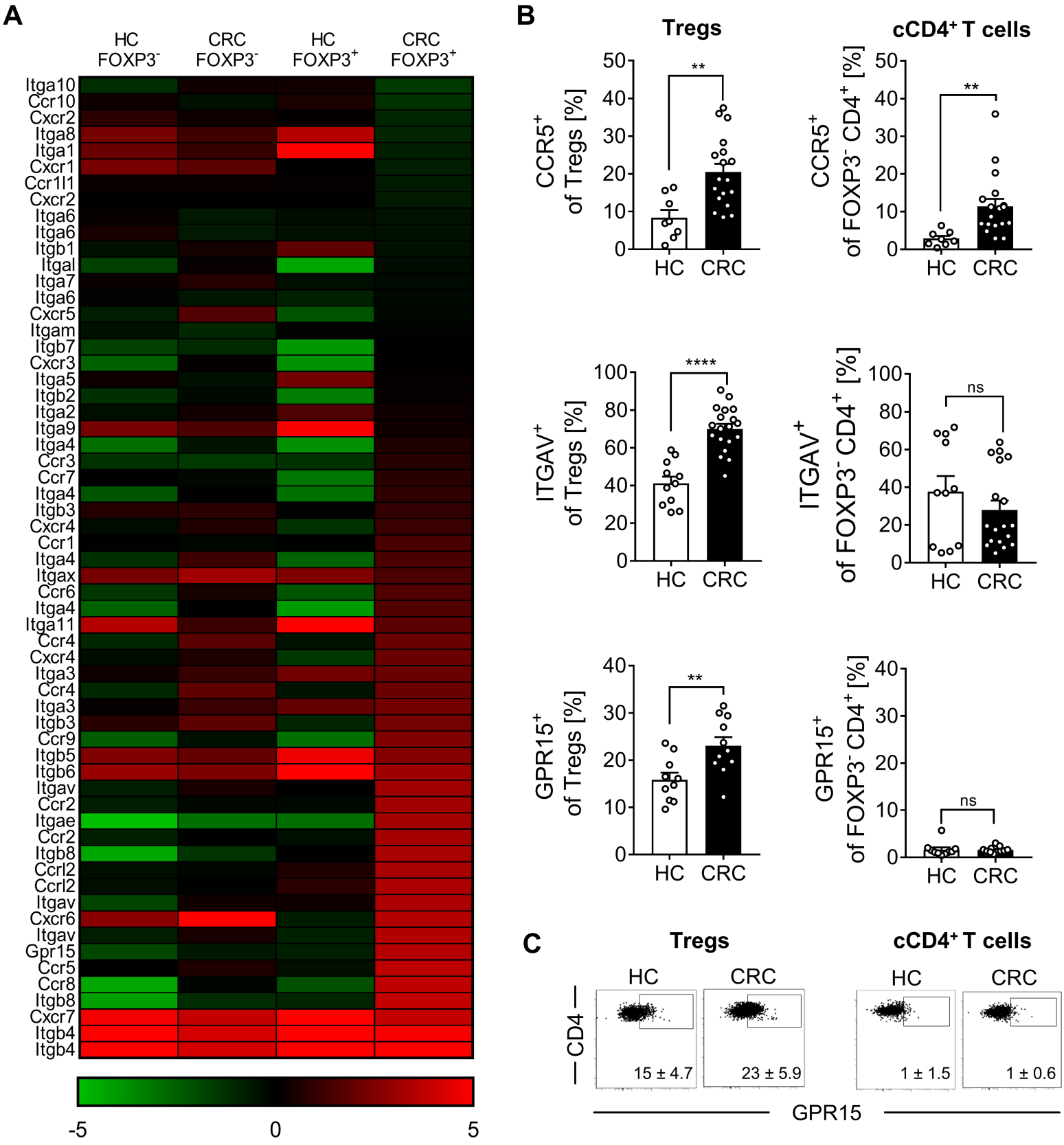

Adamczyk et al., Figure 4

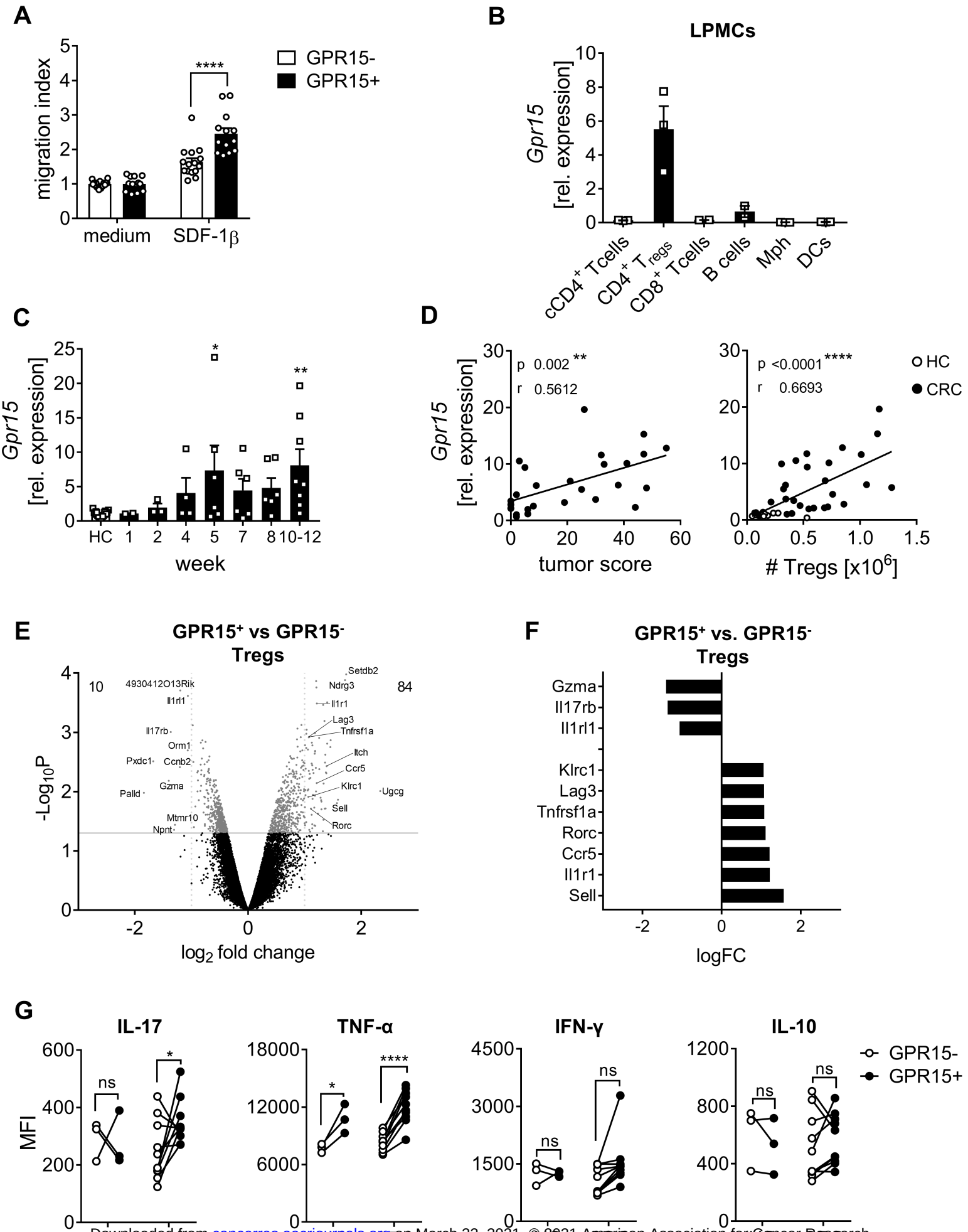

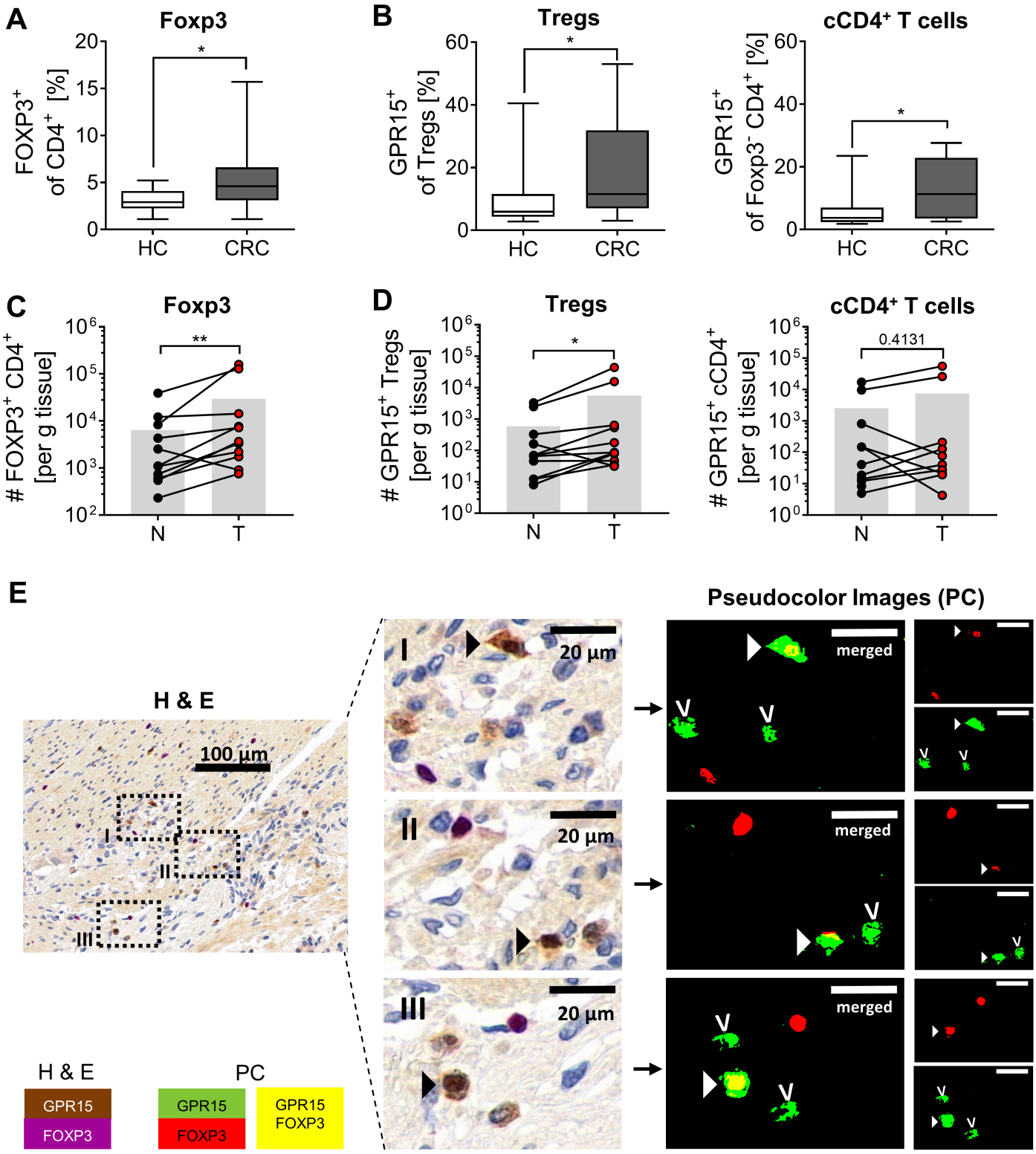

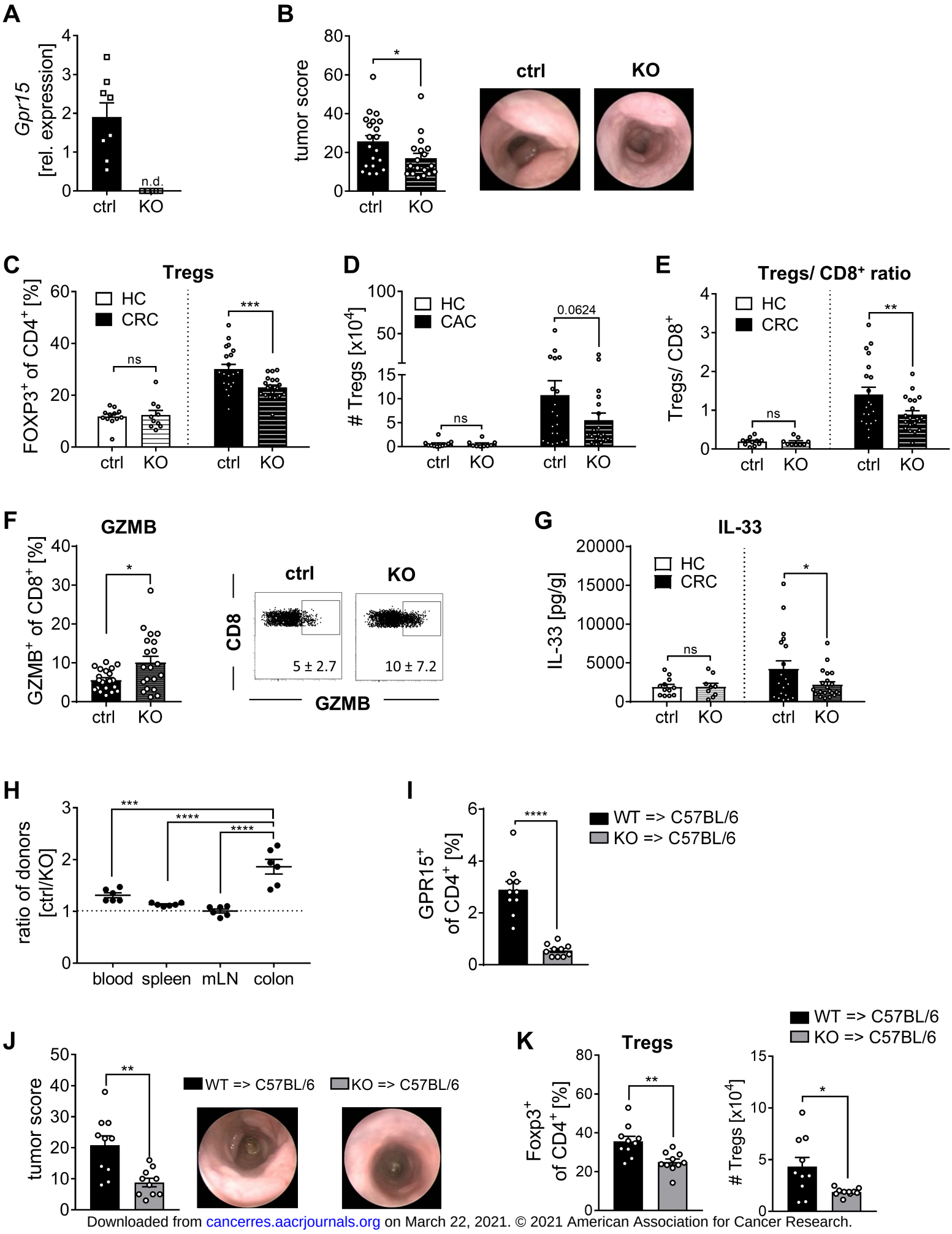

AACR American Association for Cancer Research

Cancer Research

The Journal of Cancer Research (1916–1930) | The American Journal of Cancer (1931–1940)

GPR15 facilitates recruitment of regulatory T cells to promote colorectal cancer

Alexandra Adamczyk, Eva Pastille, Jan Kehrmann, et al.

Cancer Res Published OnlineFirst March 16, 2021.